APPLIED ORGANOMETALLIC CHEMISTRY
Appl. Organometal. Chem. 2006; **20**: 81–88
Main Group Metal Compounds
Published online 28 October 2005 in Wiley InterScience (www.interscience.wiley.com). DOI:10.1002/aoc.1006

The use of alumatrane for the preparation of high-surface-area nickel aluminate and its activity for CO oxidation

K. Utchariyajit[1], E. Gulari[2] and S. Wongkasemjit[1]*

[1]The Petroleum and Petrochemical College, Chulalongkorn University, Bangkok 10330, Thailand
[2]Department of Chemical Engineering, University of Michigan, Ann Arbor, MI 48109-2136, USA

Received 10 June 2005; Revised 4 July 2005; Accepted 13 September 2005

Supported nickel has been used in a wide range of applications for industrial reactions, such as steam reforming, hydrogenation and methanation. In this work, nickel aluminate was prepared by the sol–gel process using alumatrane as the alkoxide precursor, directly synthesized from the reaction of inexpensive and available compounds, aluminum hydroxide and TIS (triisopropanolamine) via the oxide one pot synthesis (OOPS) process. Various conditions of the sol–gel process, such as pH, calcination temperature, hydrolysis ratio and ratio of nickel to aluminum, were studied. All samples were characterized using FTIR, TGA, XRD, TPR, DR-UV and BET. The BET surface area was in the range of 340–450 m^2/g at the calcination temperature of 500 °C with a mesoporous pore size distribution. Catalyst activity testing in CO oxidation reaction depended on Ni : Al ratio and calcination temperature. Higher activity was obtained from higher Ni content and lower calcination temperature. In addition, catalysts prepared using alumatrane precursor had higher percentage conversion than those prepared using aluminum hydroxide precursor. Copyright © 2005 John Wiley & Sons, Ltd.

KEYWORDS: alumatrane; nickel aluminate; sol–gel process

INTRODUCTION

Metal oxide catalysts are widely used in industry, especially the petrochemical industry. Ni-based catalysts have been intensively studied due to their low cost. Commonly used supports are silica, MCM-41[1] or alumina. Several studies of alumina-supported nickel catalysts[2,3] prepared by co-precipitation[3] (SA 110–200 m^2/g) or by the sol–gel process (SA 200–300 m^2/g)[2] have revealed the formation of nickel aluminate spinel, $NiAl_2O_4$, a stable compound with strong resistance to acids, alkalis, and having high melting point and surface area. More importantly, nickel aluminate is capable of resistance to deactivation by coke formation.[4]

Traditionally, dry mixing of ceramics and metal powders obtained by heat treatment is difficult to control and results in non-uniform dispersion of the components. In contrast, the sol–gel process offers several advantages, such as low cost and ability to control the size and morphology of products. In addition, materials of specifically macroscopic morphology can be easily designed, such as ultra-fine particle, fiber, thin film and monolith. The sol–gel process is performed at low temperature followed by appropriate heat treatment. It provides not only uniform microstructure with a high degree of dispersion between the metal and ceramic phases,[5] but also high product purity. Owing to the hydrolysis reaction involved in the sol–gel process, water induces so-called 'sol', subsequently condensed to metal oxide network, leading to a gel formation. Parameters in the sol–gel process, such as pH, proportion of water used for the hydrolysis and the presence of either acid or base catalyst,[6] are important. Calcination temperature and duration of calcination also have a significant impact on the final structure and texture of products, especially in the case of nickel aluminate spinel. An increase in calcination temperature results in a development of crystalline of $NiAl_2O_4$.[4]

Generally, commercially available aluminum alkoxides, such as aluminum *sec*-butoxide or aluminum isopropoxide,

*Correspondence to: S. Wongkasemjit, The Petroleum and Petrochemical College, Chulalongkorn University, Bangkok 10330, Thailand.
E-mail: dsujitra@chula.oc.th

are used as ceramic precursors due to the purity of starting materials and the low temperature for a reaction to occur. However, they are expensive and have low hydrolytic stability, resulting in uncontrollable reactions. These problems have been resolved by synthesis of simple alkoxide precursors containing one or more bulky alkoxide ligands, causing them to be more hydrolytically stable due to the obstruction of coordination site on the metal. Aluminum hydroxide can be used as a precursor for the preparation of these aluminum alkoxides, but the gelation of aluminum hydroxide occurs rapidly. It is thus difficult to obtain a uniform gel. This problem can be solved by slowing down the precursor's reactivity by using either a strong mineral acid[7] or a chelating agent, such as triisopropanolamine (TIS), to form alumatrane complexes.[8] In this work, alumatrane was used as an alkoxide precursor for loading nickel onto alumina by means of the sol–gel process. Optimal conditions to obtain high surface area and the highest activity for CO oxidation reaction catalysis were investigated.

EXPERIMENTAL

Materials

Aluminum hydroxide hydrate [$Al(OH)_3.xH_2O$] was purchased from Sigma Chemical Co. Triisopropanolamine [TIS, $N(CH_2CHCH_3OH)_3$] and nickel acetate [$(CH_3COO)_2Ni$], obtained from Aldrich Chemical Co. Inc. (USA), were used as received. Ethylene glycol (EG, $HOCH_2CH_2OH$) from J.T. Baker Inc. (Phillipsburg, USA) was used as a solvent for the alumatrane synthesis. Acetonitrile (CH_3CN) and methanol (CH_3OH) were obtained from Lab-Scan Company Co. Ltd and distilled before use. Nitric acid and ammonia solution, used to adjust pH in the sol–gel process, were purchased from Lab-Scan Company Co. Ltd, and used as received.

Materials characterization

Functional groups of materials were followed using FTIR spectrophotometer (Nicolet, Nexus 670) with 16 scans at a resolution of 4 cm^{-1}. Thermogravimetric analysis (TGA) was carried out on TG-DTA (Pyris Diamond Perkin Elmer) with a heating rate of 10 °C/min from room temperature to 750 °C under nitrogen atmosphere to determine the thermal stability of alumatrane. Powder X-ray diffraction (PXRD) patterns were carried out to characterize crystallinity of samples using a Rigaku X-ray diffractometer with Cu$K\alpha$ as a source. Diffused reflectance UV–vis spectra were collected on a Shimadzu UV 2550–visible spectrophotometer in the range 190–900 nm. The reducibility was investigated by temperature-programmed reduction on TPD/R/O/MS Themo Finnigan 1100. The reducing gas was 5% H_2 in N_2 at a flow rate of 40 ml/min and a heating rate of 10 °C/min. The BET surface area, pore volume and pore size distribution were measured on Autusorb-1 gas sorption system (Quantasorb JR) using nitrogen at 77 K. Samples were degassed at 250 °C under a reduced pressure prior to measurement. The morphology was studied on Jeol 5200-2AE scanning electron microscope.

Synthesis of alumatrane

Following the method described by Opornsawad *et al.*,[8] alumatrane was synthesized directly from inexpensive and widely available starting materials via the oxide one pot synthesis (OOPS) process, which is the one-step reaction. Aluminum hydroxide, TIS and EG were added into a 250 ml two-necked round-bottom flask. The mixture was homogeneously stirred at room temperature before heating to 200 °C under nitrogen in an oil bath for 10 h. Excess EG was removed under vacuum (10^{-2} Torr) at 110 °C to obtain crude product. The crude solid was washed with acetonitrile and dried under vacuum at room temperature.

Synthesis of nickel aluminate via sol–gel process

Nickel aluminate was synthesized using alumatrane and nickel acetate precursors via the sol–gel process at various Ni : Al ratios, pH, hydrolysis ratios and calcination temperature. Alumatrane and nickel acetate were dissolved in methanol for 1 h before adding water and adjusting pH. The pH value of the unadjusted mixture solution was 9. Thus, for acid conditions, pH 3, 5 and 7, HNO_3 was used whereas NH_4OH was added for obtaining pH 11. Three hydrolysis ratios of 9, 18 and 27, were chosen, following the result of a previous work.[6] The solution was vigorously stirred at room temperature, followed by heat treatment of the resulting gels at calcination temperature ranging from 500 to 900 °C and held at the final temperature for 7 h.

Activity study on CO oxidation reaction

The catalytic tests of CO oxidation with O_2 were carried out in a fixed-bed flow reactor at a temperature ranging from 200–450 °C with 180 ml/min total gas flow and a feeding mixture of CO–O_2–He (1–2–97%) with 27 000 GHSV; 0.2 g of catalyst was employed for each experiment.

RESULTS AND DISCUSSION

Effects of Ni : Al ratio and of calcination temperature

Figure 1 shows XRD patterns of three different nickel to alumina ratios (Ni : Al), which began to crystallize at 500 °C. For the Ni : Al ration of 1 : 2 calcined at 500 and 600 °C, the peak at around 45° appeared as a wide band at a slightly lower angle than for the other samples calcined at higher temperature. This could indicate the presence of a small amount of NiO besides $NiAl_2O_4$ due to the main peaks of NiO phase, according to JCPDS 4–835 as follows: 37.29 ($I/I_0 = 100\%$), 43.30 (100%) and 62.91 (57%) for NiO phase. As the temperature increased, the product crystallinity also increased and corresponded to JCPDS 10–339 for $NiAl_2O_4$ phase along with the change in catalyst color from greenish

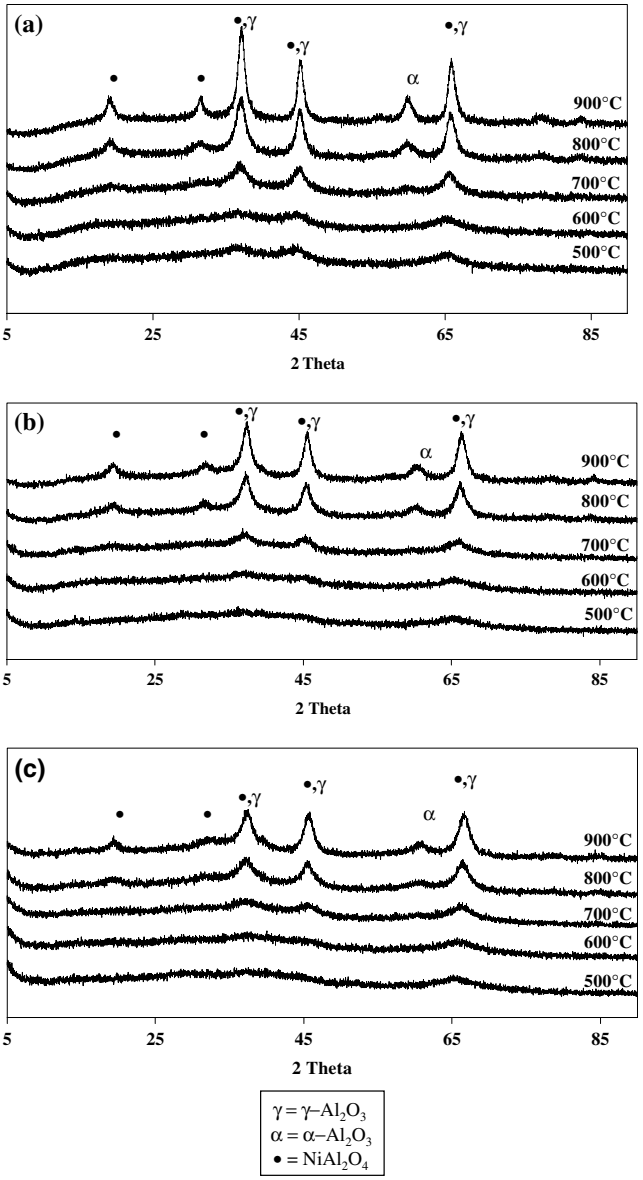

Figure 1. XRD patterns of the samples prepared at pH 9, hydrolysis ratio 9 and calcined at various calcination temperature with a Ni : Al mole ratio of (a) 1 : 2, (b) 1 : 4 and (c) 1 : 8.

to light blue. The samples calcined at 800 and 900 °C showed some part of γ-Al_2O_3 transform to α-Al_2O_3[9] evidenced by the peak at 57°. According to the JCPDS file, the XRD pattern corresponding to nickel aluminate phase should provide three major peaks at 37.01° ($I/I_0 = 100\%$), 45.00° ($I/I_0 = 65\%$) and 65.54° ($I/I_0 = 60\%$). However, the peaks of γ-Al_2O_3 and $NiAl_2O_4$ phases overlapped. The relative intensities (I/I_0) of the peaks at 2θ values of 37 and 45° were thus used to identify the characteristics of the samples. The $NiAl_2O_4$ phase generally gives peak intensities of 100 and 60–65%, whereas the Al_2O_3 phase intensities are 80 and 100%, respectively. The lower Ni : Al ratio seemed to give the formation of solid solution Al_2O_3 and $NiAl_2O_4$. The crystallinity of $NiAl_2O_4$ phase was slightly improved with the increase in the Ni : Al ratio due to an increasing ratio of Ni : Al; the relative intensity of XRD patterns were closer to nickel aluminate phase. As expected, owing to the actual ratio of $NiAl_2O_4$ spinel (Ni : Al = 1 : 2), when the Ni : Al ratio was low, there was not enough Ni to form a complete $NiAl_2O_4$ spinel; the excess Al from alumatrane, thus, arranged itself and became Al_2O_3.[1]

FTIR spectra of the samples (Fig. 2) prepared using various Ni : Al ratios and calcined at various calcination temperatures show two bands at 3000–3700 and 1300–1700 cm^{-1} corresponding to the stretching and bending vibrations, respectively, of the O–H bonds of water contained in the samples. The IR bands observed below 1000 cm^{-1} can be attributed to the stretching vibrations of M–OH modes (M = Ni, Al). These bands are related to the M atoms presenting both octahedral and tetrahedral sites. The characteristic of $NiAl_2O_4$ is clearly identified in the sample calcined at 800 and 900 °C, showing the bands at 740 and 505 cm^{-1}.[4] The adsorption band at 740 cm^{-1} was assigned to the stretching vibrations of tetrahedral (MO_4). The presence of the stretching vibrations of octahedral (MO_6) is illustrated by the absorption band at 505 cm^{-1}. The preparation conditions and calcination temperature have a significant impact on the final structure and texture of nickel loaded alumina.

Effects of pH and hydrolysis ratio

XRD patterns showed no significant difference for the samples prepared using various hydrolysis ratios at different

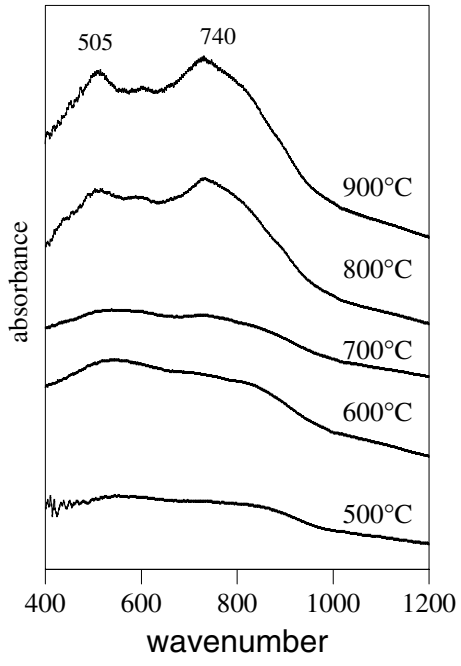

Figure 2. FTIR spectra of the samples (Ni : Al = 1 : 2) calcined at various calcination temperatures.

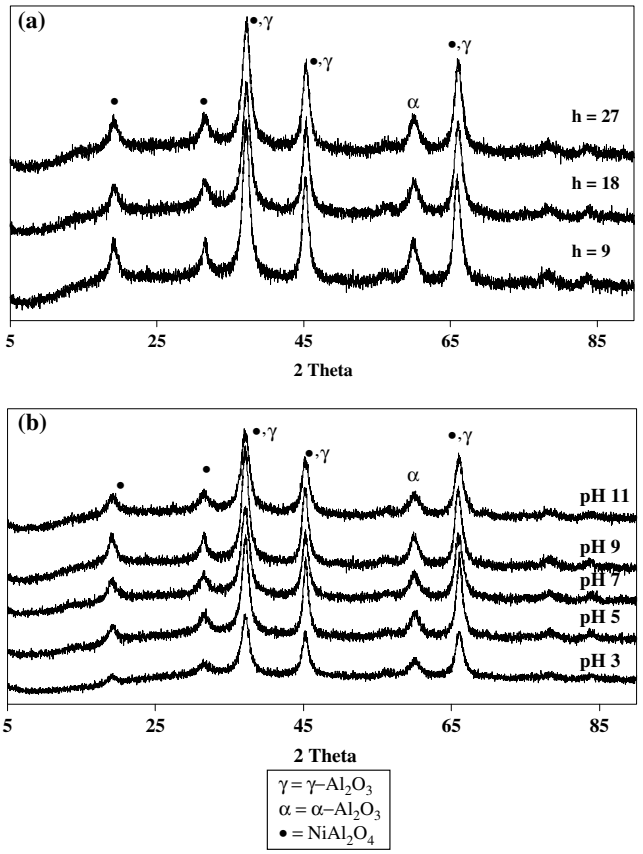

Figure 3. XRD patterns of the samples (Ni : Al = 1 : 2) calcined at 900 °C using (a) various hydrolysis ratios and (b) various pHs.

calcination temperature, as shown in Fig. 3(a), presenting the XRD patterns of the samples calcined at 900 °C. However, pH seems to affect the product phase. Figure 3(b) shows XRD spectra of samples prepared in different pH solutions, followed by calcination at 900 °C. The samples prepared at the lowest (3) or the highest (11) pH showed lower intensity compared with the others obtained at intermediate pHs. This phenomenon could be explained in terms of the reactions involved in the sol–gel process, hydrolysis and condensation reactions. Instead of condensation precursors, octahedral aluminate $[Al(OH_2)_6]^{3+}$ species were observed below pH 3. Similarly, above pH11, $[Al(OH)_4]^-$ were formed.[10] In addition, it is well known that both acidic and basic species accelerate the sol–gel process, thus too much acid or base increases the rate of hydrolysis compared with condensation resulting in smaller and less ordered aggregates which do not crystallize as well as the larger and more ordered aggregates. However, all the samples from these XRD results indicate only the formation of nickel aluminate. Nickel oxide phase is not seen.

The FTIR spectra of $NiAl_2O_4$ prepared using various hydrolysis ratios and pHs after calcination at 900 °C (not shown) show the same pattern as Fig. 2. The effect of Ni : Al ratio could be observed in Fig. 4, with increased intensities of

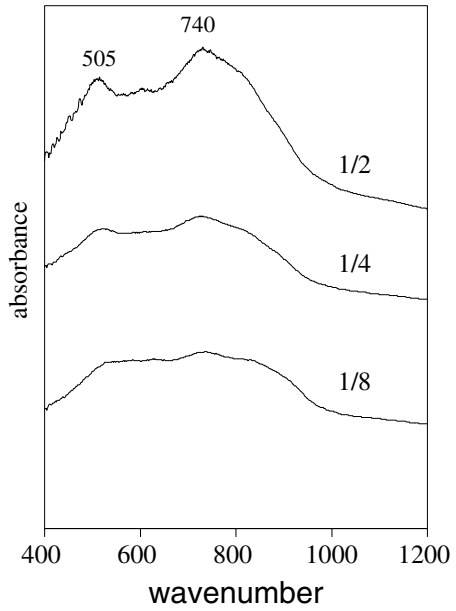

Figure 4. FTIR spectra of the samples prepared using various Ni : Al ratios and calcined at 900 °C.

the bands below 1000 cm^{-1} belonging to M–O–M stretching with increasing ratio of Ni : Al.

Reducibility and structure of Ni aluminate spinel

TPR was carried out to confirm the above results and to investigate the reducibility of the corresponding nickel aluminate spinel. As shown in Fig. 5, the TPR profile of the catalyst calcined at 500 °C showed the maximum reduction temperature (T_M) at 573 °C, which is higher than the reduction[11] of bulk nickel oxide (T_M = 350 °C), indicating a strong interaction between nickel and alumina providing that the $NiAl_2O_4$ was formed.[3] The effect of calcination temperature on the reduction profiles also shows that the increase in calcination temperature makes the reduction increasingly more difficult, as inferred from the shift of

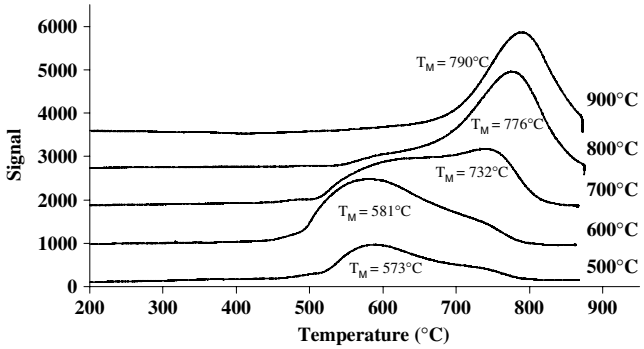

Figure 5. TPR profiles of the 1 : 2 Ni : Al ratio at various calcination temperatures.

the main reduction peak and the T_M value to higher temperature. The reduction of Ni^{2+} species on alumina which begin to crystallize in the sample calcined at 500–600 °C occurred at lower temperatures ($T_M \leq 600$ °C) due to the larger crystallites sizes and the stronger interaction between Ni and Al with increasing calcination temperature, causing the reduction process to go slower. These results are similar to those obtained by Cesteros *et al*.[12] and Pena *et al*.[4] The sample calcined at 700 °C shows the overlap of two reduction peaks due to the presence of both γ-Al_2O_3 to α-Al_2O_3.

The influence of Ni loading [Fig. 6(a)] on reducibility showed that T_m decreases with increasing Ni loading. At low nickel content, Ni could be stabilized at the vacancies of α-alumina with defective spinel structure,[13] resulting in a higher reduction temperature.

The effects of hydrolysis ratio and pH are given in Fig. 6(b and c). The reducibility of nickel aluminate prepared at various hydrolysis ratios and pHs was not significantly different.

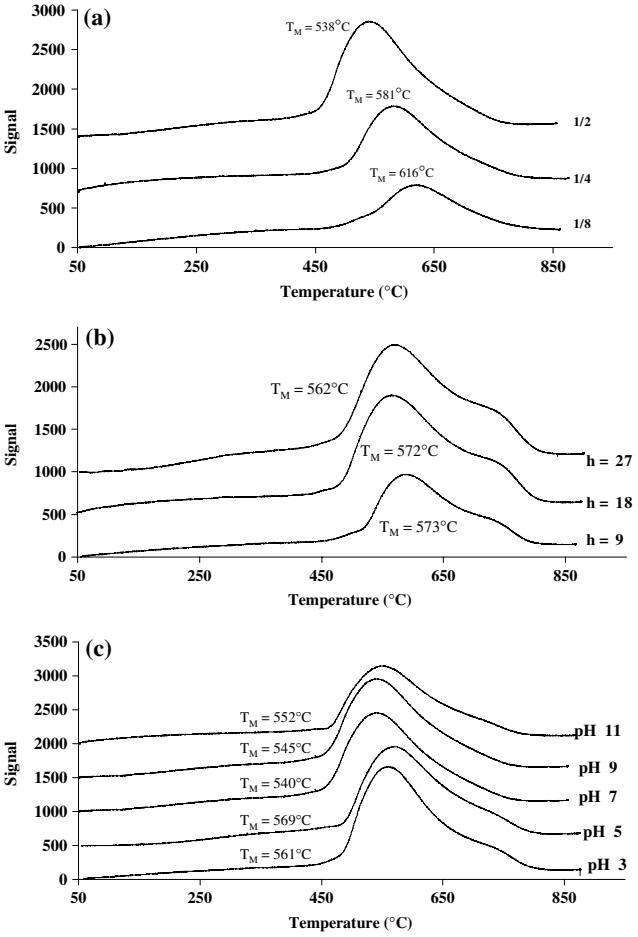

Figure 6. TPR profiles of the samples calcined at 500 °C at (a) various Ni : Al ratios, (b) various hydrolysis ratios and (c) various pHs.

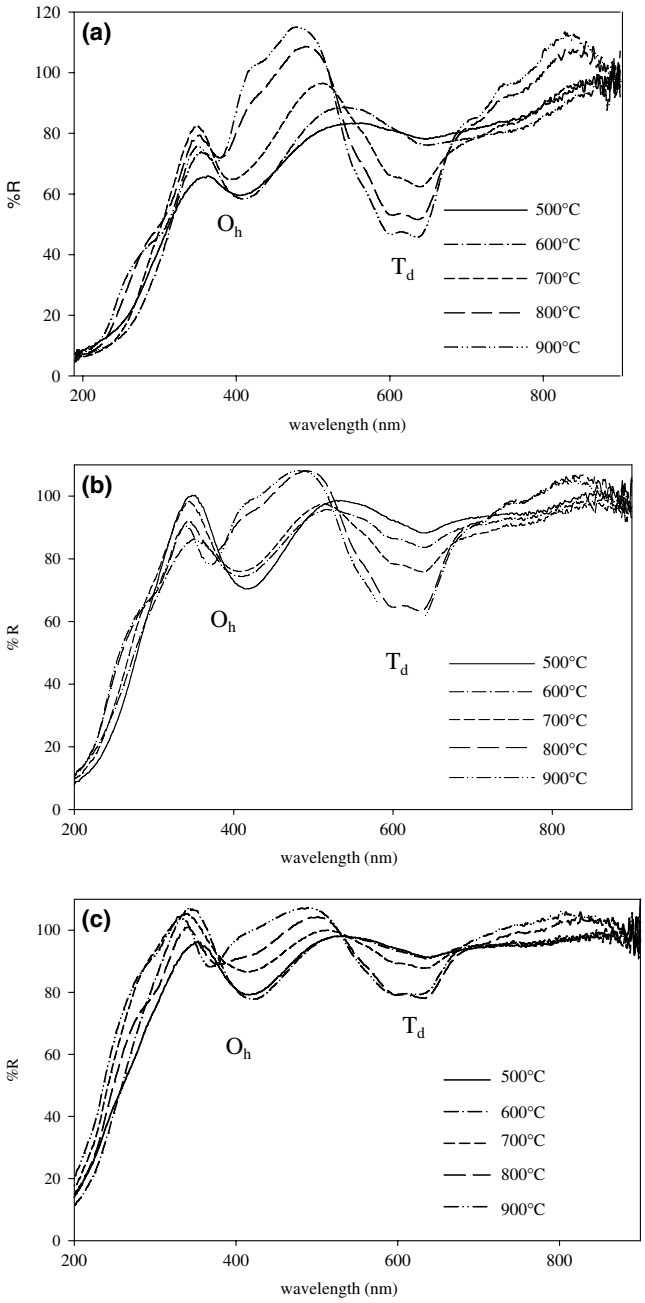

Figure 7. DR-UV spectra of the samples calcined at various calcination temperatures and a Ni : Al ratio of (a) 1 : 2, (b) 1 : 4 and (c) 1 : 8.

To confirm the identity of nickel species and the formation of nickel aluminate, DR-UV analysis was conducted, as shown in Fig. 7. Characteristic bands in the regions of around 370–410 and 600–645 nm were observed, indicating that in all samples nickel aluminate spinel phase was formed. These two bands indicate the distribution of Ni(II) ions among, respectively, octahedral and tetrahedral sites of alumina lattices in a spinel structure.[14] The Ni(II) ions entering into the Al_2O_3 lattices simultaneously occupied tetrahedral

and octahedral sites. The ratio depends on the calcination temperature. The higher the calcination temperature, the higher the tetrahedral to octahedral ratio. This is most likely due to the fact that, at the higher calcination temperatures, the structure collapsed, destroying more octahedral sites. It is worth noting that the peaks around 400 nm of the samples calcined at 800 and 900 °C were shifted to lower wavelengths due to the phase transformation of γ-Al_2O_3 to α-Al_2O_3. These results are in agreement with the results from XRD and FTIR. As expected, when increasing the ratio of nickel to alumina, more Ni(II) ions diffused into alumina lattices at both octahedral and tetrahedral sites, while there was no significant difference for the samples prepared at various pHs and hydrolysis ratios during the sol–gel process.

BET surface area results

BET surface areas determined are listed in Tables 1–3. It can be seen that the catalysts prepared in this investigation have much larger specific surface areas than the results reported previously for the Ni/Al_2O_3 catalysts obtained by other precursors via the sol–gel process (SA 200–300 m^2/g)[2,15] or by the co-precipitation method (SA 110–200 m^2/g)[3,16] at the same calcination temperature (500 °C). Even higher calcination temperatures in this work gave higher surface areas than the co-precipitation method (SA 94 m^2/g) for the sample calcined at 900 °C.[16] All samples showed similar pore size distributions (Fig. 8) in the mesoporous region having pore diameters around 3–6 nm.

Table 1. BET analysis of the samples prepared at pH 9 and calcined at various calcination temperature

Condition	Surface area (m^2/g)
1 : 2 Ni : Al 500 °C	410
1 : 2 Ni : Al 600 °C	272
1 : 2 Ni : Al 700 °C	260
1 : 2 Ni : Al 800 °C	174
1 : 2 Ni : Al 900 °C	140

Table 2. BET analysis of the samples calcined at 500 °C and various pHs

Condition	Surface area (m^2/g) ($h = 9$)	Surface area (m^2/g) ($h = 18$)
1 : 2 Ni : Al pH 3	340	337
1 : 2 Ni : Al pH 5	360	366
1 : 2 Ni : Al pH 7	392	348
1 : 2 Ni : Al pH 9	410	422
1 : 2 Ni : Al pH 11	380	350

Table 3. BET analysis of the samples prepared at pH 9 and calcined at 500 °C using various hydrolysis ratios

Condition	1 : 2 Ni : Al	1 : 4 Ni/Al	1 : 8 Ni : Al
$h = 9$	410	381	377
$h = 18$	422	452	402
$h = 27$	375	416	393

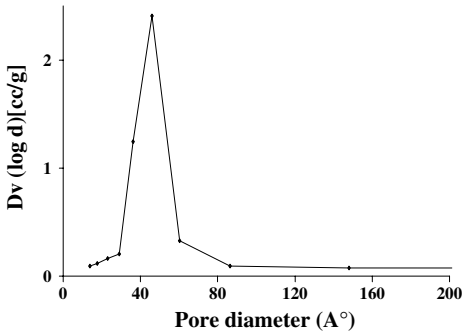

Figure 8. Pore size distribution of the samples (Ni : Al = 1 : 2) prepared at $h = 9$, pH 9 and calcined at 500 °C.

The Ni content did not have a significant effect on the surface area, giving around 410–450 m^2/g, indicating that the nickel metal was uniformly distributed in the final product and did not accumulate on the surface.[17] As expected, with increasing calcination the surface area decreased from 410 to 140 m^2/g due to an increase in crystallinity as the calcination temperature increased from 500 to 900 °C. Table 2 shows that the highest surface area was obtained at the pH of the isoelectric point of the system[6] where a three-dimensional gel network had a suitable time to form. Other pHs may drive the hydrolysis and condensation reactions to go either too fast or too slow, resulting in lower surface area. Similarly, the effect of hydrolysis ratio shown in Table 3 indicated that the sample prepared using an appropriate amount of water gave a higher surface area. In this case, the hydrolysis ratio of 18 showed the highest value, as compared with other hydrolysis ratios. Again, low hydrolysis ratio, implying less water, led to more difficult hydrolysis, which consequently limited the condensation step. Thus, a higher water : alkoxide ratio would result in a greater extent of hydrolysis and condensation reactions.[18] However, too much water added during the sol–gel process would give faster hydrolysis than condensation, resulting in less branched linear chains.

SEM results

SEM results showing the morphologies of the samples calcined at 500 and 700 °C in Fig. 9 are in good agreement with the XRD results. That is, the higher the calcination temperature, the higher the crystallinity.

Catalytic study of nickel aluminate

The catalytic activity test on CO oxidation reaction with O_2 showed the temperature dependence on the conversion of CO oxidation reaction (Fig. 10). It was found that the activities depend on the ratio of nickel to alumina, calcination

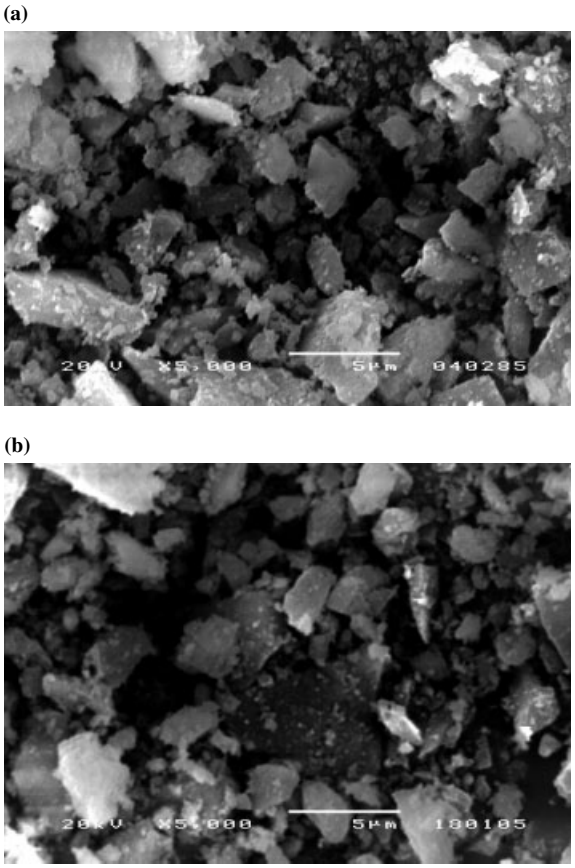

Figure 9. SEM micrographs of the samples calcined at (a) 500 and (b) 900 °C.

temperature and type of precursors. The activity increased with the increase in the nickel content [Fig. 10(a)], resulting in more active sites of Ni occupied for the oxidation reaction. The activity also increased as the calcination temperature decreased due to the higher surface area of the catalyst [Fig. 10(b)].

Further study of the catalyst activities was carried out with different aluminum sources [Fig. 10(c)]. The sample synthesized from alumatrane precursor was more active than that produced by $Al(OH)_3$ precursor. This is probably due to the purer and more homogeneous nickel aluminate obtained from alumatrane precursor, giving better Ni ions distribution in alumina phase. As mentioned previously, $Al(OH)_3$ forms gel easily,[6] thus being unable to control the sol–gel process condition, giving a NiO phase in addition to a nickel aluminate phase.

CONCLUSIONS

Alumatrane synthesized from inexpensive and available compounds via the one-step process was successfully used as an alkoxide precursor for preparing nickel-loaded alumina via the sol–gel route followed by heat treatment. The calcined

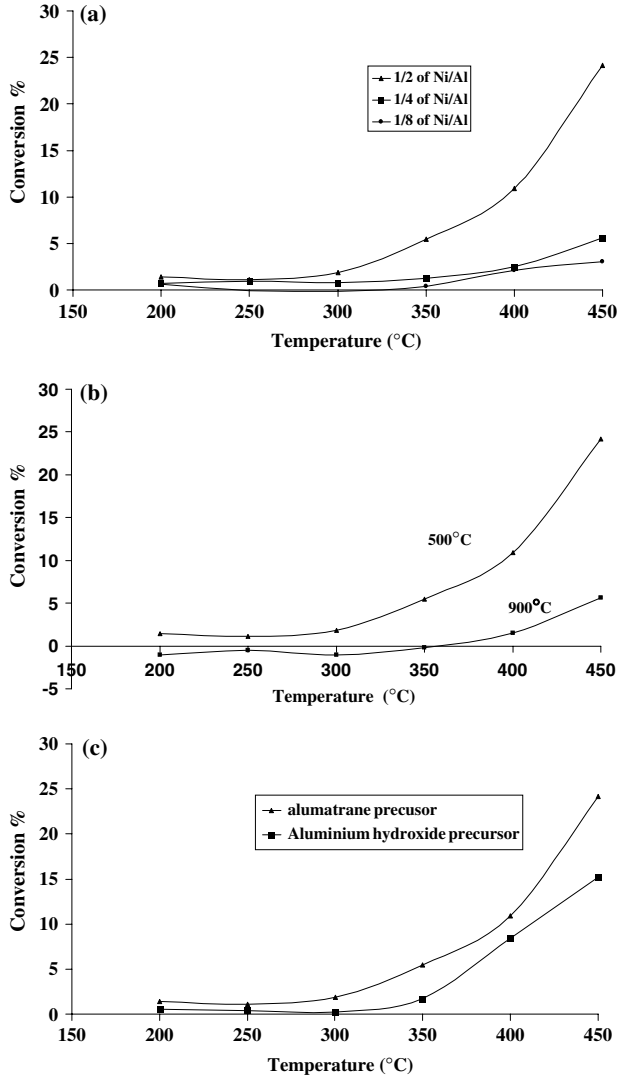

Figure 10. Activity testing of the samples using (a) various Ni : Al ratios, (b) various calcination temperatures and (c) different precursors (Ni : Al = 1 : 2 and calcined at 500 °C.

samples favored the formation of nickel aluminate spinel, $NiAl_2O_4$, confirmed using XRD, FTIR, TPR and DR-UV. The calcination temperature and the nickel content affected the crystallinity of the samples. Higher crystallinity resulted from higher calcination temperature and nickel content. BET surface areas were found to be in the range 300–450 m^2/g at a calcination temperature of 500 °C. Higher CO oxidation catalysis activity was obtained from catalysts with higher Ni content and lower calcination temperature. Catalysts prepared using alumatrane precursor had higher percentage conversion than those prepared from aluminum hydroxide.

REFERENCES

1. Jia J, Wang Y, Eishi T, Shishido T, Takehira K. *Microporous Mesoporous Mater.* 2003; **57**: 283–289.

2. Arean CO, Mentruit MP, Lopez AJ, Parra JB. *Colloids Surf. A: Physicochem. Engng Asp.* 2001; **180**: 253–258.
3. Xu Z, Li Y, Zhang J, Chang L, Zhou R, Duan Z. *Appl. Catal. A: Gen.* 2001; **210**: 45–53.
4. Pena JA, Herguido J, Guimon C, Monzon A, Santamaria J. *J. Catal.* 1996; **159**: 313–322.
5. Rodeghiero ED, Moore BC, Wolkenberg BS, Wulthenow M, Tse OK, Giannelis EP. *Mater. Sci. Engng* 1998; **A244**: 11–21.
6. Ksapabutr B, Gulari E, Wongkasemjit S. *Colloids Surf. A: Physicochem. Engng Asp.* 2004; **233**: 145–153.
7. Suh DJ, Park TJ, Lee SH, Kim KL. *J. Non-Crystalline Solids* 2001; **285**: 309–316.
8. Opornsawad Y, Ksapabutr B, Wongkasemjit S, Laine RM. *Eur. Polym. J.* 2001; **37**: 1877–1885.
9. Kis E, Marinkovic-Neducin R, Lomic G, Boskovic G, Obadovic DZ, Kiurski J, Putanov P. *Polyhedral* 1998; **17**: 27–34.
10. Livage J. *Catal. Today* 1998; **41**: 3–19.
11. Negrier F, Marceau E, Che M, Caro D. *C. R. Chim.* 2003; **6**: 231–240.
12. Cesteros Y, Salagre P, Medina F, Sueiras JE. *Appl. Catal. B: Environ.* 2000; **25**: 213–227.
13. Molina R, Poncelet G. *J. Catal.* 1998; **173**: 257–267.
14. Jitianu M, Jitianu A, Zahaarescu M, Crisan D, Marchidan R. *Vibr. Spectrosc.* 2001; **22**: 75–86.
15. Piao L, Li Y, Chen J, Lin JY. *Catal. Today* 2002; **74**: 145–155.
16. Chokkaram S, Srinivasan R, Milburn DR, Davis BH. *Mol. Catal. A: Chem.* 1997; **121**: 157–169.
17. Suh DJ, Park TJ, Kim JH, Kim KL. *J. Non-Crystalline Solids* 1997; **225**: 168–172.
18. Pascual ER, Larrea A, Monzon A, Gonzalez RD. *J. Solid-St. Chem.* 2002; **168**: 343–353.

